JNTM JOURNAL of NEW TECHNOLOGY and MATERIALS

Journal of New Technology and Materials

Vol. 14, No. 2 (2024), 09–20

RESEARCH ARTICLE

Ligand-Gated Orthogonal Probe Mapping of Site Accessibility in Nickel–Gallium Superatom Cluster Ensembles

Jiacheng Fang[1], Ray H. Baughman[2,*] and Song-Zhi Liu[1]

[1]Department of Material Functions and design, Nagoya Institute of technology, Gokiso-Cho Showa-ku, Nagoya, Aichi, 466-8555 Japan. [2]NanoTech Institute, University of Texas at Dallas, 800 West Campbell road, Richardson, TX75080, 75080 USA

*Correspondence: ray.baughman@utdallas.edu

Received date: January 13, 2024; Accepted date: October 18, 2024

Abstract

Nickel–gallium intermetalloid superatom clusters offer models of precise elemental atomic arrangements in composition-dependent mixed-metal assemblies; however, their interpretation becomes challenging in the case where several isobaric species are present within a single ligand-protected complex. In this work, the ligand-gated orthogonal probe mapping (LGOPM) strategy is applied to the series of intermetalloid clusters $Ni_{6+x}Ga_{6+y}(Cp^*)_6$ with $x + y \leq 2$. The analysis utilizes the invariant $(NiCp^*)_6$ cage as a starting point with two independently defined probes, used to discriminate between accessible and protected inner-shell atoms. The main objective of this study is to determine whether it is possible to translate a mixture of isobaric Ni–Ga clusters into a resolution in terms of nickel and gallium site accessibility. The answer to this question is positive since carbon monoxide reaction allows one to select nickel-accessible compositions while the application of triisopropylsilyl acetylene photodissociation leads to isolation of the gallium derivatizable cluster. Thus, in the descriptor matrix, the Ni_6Ga_6 and Ni_6Ga_7 clusters belong to the group of cage-protected molecules; the Ni_7Ga_6 and Ni_7Ga_7 clusters belong to the class responding to carbon monoxide treatment while the Ni_8Ga_6 cluster represents the photochemical gallium-labile molecule. Interpretations follow the major equations, figures, and tables, connecting indices, masses, spectroscopic, magnetism, and probe parameters with chemical phenomena.

Keywords: nickel–gallium clusters, intermetalloid materials, superatom complexes, ligand-shell gating, site accessibility, carbon monoxide, alkynyl derivatization, LIFDI mass spectrometry

1 Introduction

The class of atom-precise mixed-metal clusters occupies a unique middle ground in between classical molecular coordination compounds and extended intermetallic solids. On the one hand, these species are defined by their discrete formulas, ligand environments, and spectroscopically accessible properties; on the other hand, their metallic cores may display characteristics that resemble those of nanomaterials or extended solids, such as delocalized bonding, shell-like electronic configuration, and composition-dependent reactivity. As such, ligand-protected superatom clusters have become an important tool for materials-oriented research in molecular composition space, especially in light of the sensitivity of frontier orbital composition, spin state, substrate binding properties, and stability to minor shifts in metal composition or nuclearity. While the superatom approach is particularly helpful in this context because it allows the link between cluster electron counting and electronic shell filling, ligand-protected clusters do not offer a simple extension of molecular structure with a "decorative" ligand shell; instead, they fix the coordination environment of metal sites, define the kinetic limits at which the reagent encounters reactive cores, and determine the availability of inner-core electronic states to probing [1–4].

The challenge is exacerbated by the presence of multiple metals, including elements of transition-metal or main group type. While transition metals may provide flexibility in terms of redox state, acceptor π-interaction capability, and

potential binding to organic substrates, main-group metals control electron count, polar metal-metal interaction, and electron deficiency at particular cluster sites. Such intermetalloid compositions are therefore particularly useful because they translate structural motifs characteristic for intermetallic phases into molecules that can be analyzed using techniques commonly applied in molecular science, such as X-ray diffraction, vibrational or electronic spectroscopy, mass spectrometry, and theoretical modeling [5, 6]. Unfortunately, bottom-up synthesis typically fails to provide a clean mixture with just one desired composition. Multiple cluster species with close to equal nuclearities, overlapping isotope distributions, and similar ligand shells may be produced simultaneously, rendering complete separation and isolation of each neutral cluster compound impossible or highly undesirable. The question then becomes not so much which formulas are present in the sample, but which formulas include chemically accessible sites.

Such a distinction between composition and accessibility is the key feature of the current manuscript. Indeed, even if a cluster includes nickel, this nickel may remain undetectable to a certain probe molecule, and if another composition includes gallium, this gallium may fail to react selectively. Conversely, the opposite scenario may take place, and the nickel composition may exhibit gallium-selective transformation due to specific ligand shell and core geometry. Traditional formula identification is, thus, an incomplete step unless combined with an assessment of reactivity of the cluster species in question. High-resolution mass spectrometry, isotope labeling, collision-induced dissociation experiments, solid-state nuclear magnetic resonance, vibration spectroscopy, EPR/SQUID magnetometry, and density-functional calculations may provide a variety of information, but they should be combined into a more sophisticated picture, which includes mapping of site accessibility and response.

In general, this type of analysis requires the selection of two independent probe reactions with selective detection capabilities. For example, CO may be used for nickel-based transformations, since the presence of metal-carbon interaction in addition to σ bonding depends critically on back-donation from the ligand shell. Alternatively, gallium-based selectivity can be tested using triisopropylsilylacetylene (TIPSA) as a substrate, provided that its photoactivation leads to generation of a gallium-bound alkyne product. Such approaches can be applied to the superatom cluster library with a conserved six-ligand nickel-gallium formula $Ni_{6+x}Ga_{6+y}(Cp^*)_6$, where $x + y \leq 2$. It is crucial to note that such a limitation to six nickel atoms is a strict structural constraint rather than convenient accounting tool. Thus, six nickel atoms are attributed to the shell-locking motif, while extra nickel atoms are treated as possible participants in the formation of nickel response. Accessible gallium content is similarly assessed not based on the number of gallium atoms but in accordance with the presence of selective TIPSA-related derivatives. The research question posed by this manuscript is whether the fixed shell structure allows such a complex family of mixed-metal compositions to be transformed into the map of nickel and gallium site accessibility.

The hypothesis underlying this paper is that the conserved $(NiCp^*)_6$ ligand shell may function as an internal reference system and allow CO- and TIPSA-responsive formulas to be interpreted as inner-core chemistry indicators. The manuscript tests this assumption by analyzing cluster species with respect to composition assignment, shell-conserved structure, nickel- or gallium-response, and electronic/magnetic descriptors of the difference between compositionally similar cluster compounds. By providing such an analysis explicitly, the paper identifies ligand-protected Ni–Ga superatoms as molecular materials with site-specific reactivity and creates a framework for further studies of similar cluster ensembles.

2 Materials and Methodology

2.1 Descriptor basis and data normalization

Compositional, spectroscopic, magnetic, and computed descriptors for the Ni–Ga cluster ensemble are drawn from Muhr and co-workers [7]. The cited record supplies cluster-composition assignments associated with SI Tables S2–S23, skeletal vibrational assignments associated with SI Table S1, bulk elemental-composition information associated with SI Table S24, and computed electronic-structure entries associated with SI Table S25. Only descriptors that directly constrain formula, ligand count, shell identity, inner-core site accessibility, magnetic response, and probe-dependent reactivity are used in the present analysis; supporting literature cited elsewhere remains restricted to pre-2024 publications.

All detected cluster members were normalized to the family

$$C_i = Ni_{6+x}Ga_{6+y}(Cp^*)_6, \qquad x + y \leq 2, \tag{1}$$

where $Cp^* = C_5Me_5$. Eq. 1 defines a constrained materials space rather than a broad empirical formula list. The six Cp^* groups are treated as a conserved ligand-shell constraint. This assumption is justified by the repeated six-ligand stoichiometry of the major cluster members and by the spectroscopic evidence for a dominant Cp^* environment. The descriptor-normalization step permits comparison of species with different metal nuclearities while preserving the chemical meaning of the common ligand shell.

The five-member compositional library is displayed in Figure 1. The visual comparison emphasizes that the figures are not treated as isolated molecular drawings; they define the common shell boundary and the small changes in core composition that are evaluated throughout the response-mapping procedure. In practical terms, Eq. 1 converts the

ensemble into a controlled perturbation series: changes in x and y are read against the same ligand-shell reference, so that a probe response can be assigned to altered core accessibility rather than to a changing external ligand population.

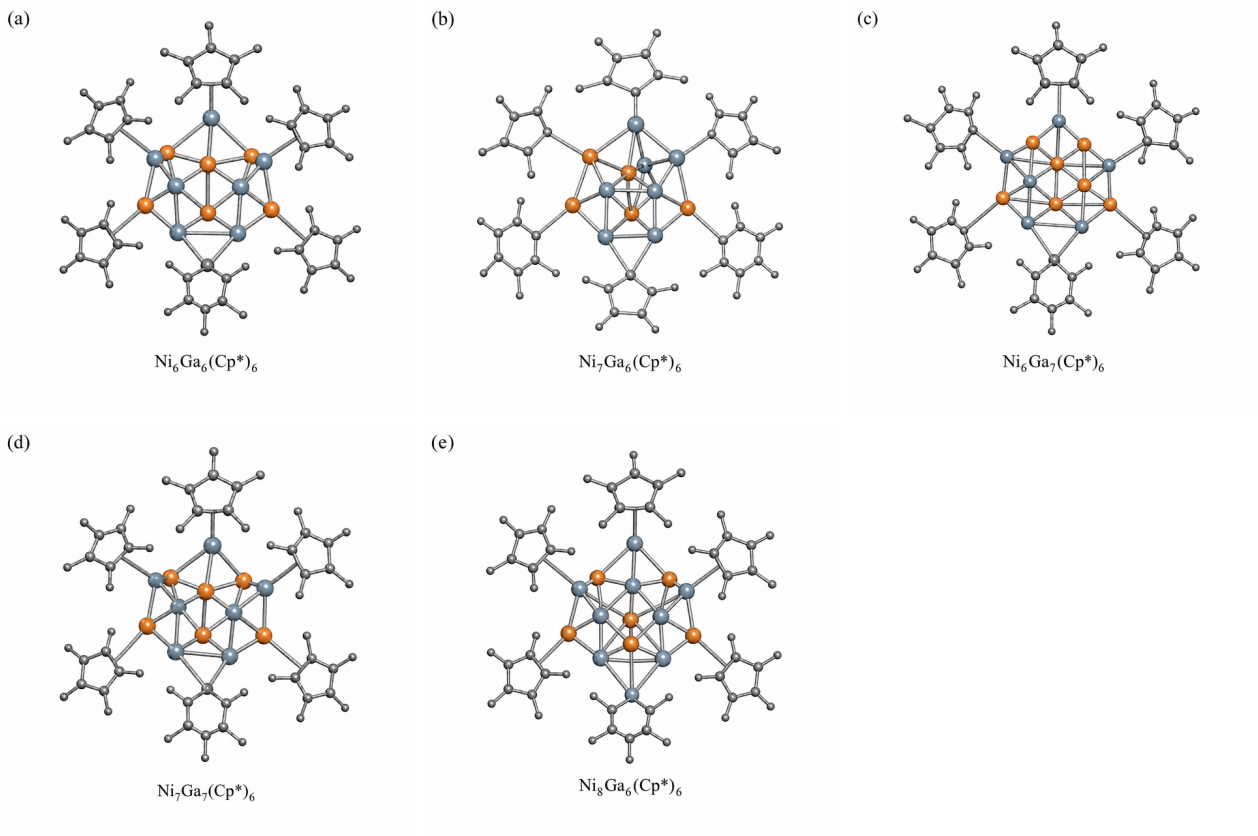

Figure 1. Representative structural views of the five normalized nickel–gallium cluster compositions used in the ligand-gated descriptor family: $Ni_6Ga_6(Cp^*)_6$, $Ni_7Ga_6(Cp^*)_6$, $Ni_6Ga_7(Cp^*)_6$, $Ni_7Ga_7(Cp^*)_6$, and $Ni_8Ga_6(Cp^*)_6$. The panels visualize the common six-ligand boundary and the core-composition changes that define the LGOPM comparison.

2.2 Ligand-gated orthogonal probe mapping

The analytical method is ligand-gated orthogonal probe mapping (LGOPM). It contains four stages. First, every cluster ion or neutral formula is rewritten in the common six-ligand representation shown in Eq. 1. Second, the six Cp^* ligands are assigned as a shell-locking motif associated with the outer nickel-bound architecture. Third, metal atoms not required by the shell are indexed as potential contributors to inner-core chemical response. Fourth, the predicted site accessibility is evaluated against two probe reactions: carbon monoxide exposure and photochemical triisopropylsilylacetylene treatment.

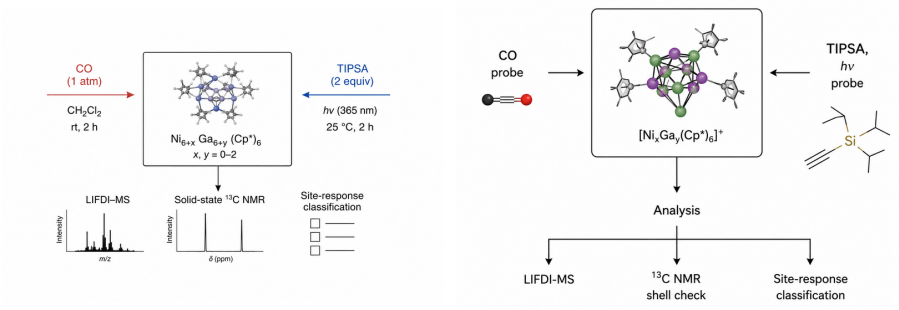

Figure 2. Orthogonal probe-mapping workflow for the Ni–Ga cluster ensemble. Carbon monoxide exposure is used to detect accessible nickel-centered response, photochemical triisopropylsilylacetylene treatment is used to identify gallium-centered derivatization, and LIFDI-MS with solid-state ^{13}C NMR provides mass-shift and ligand-shell checks before site-response classification.

The workflow in Figure 2 summarizes the method as an orthogonal sequence rather than a single-response test. The

CO and TIPSA branches are deliberately separated so that nickel-centered binding or depletion can be distinguished from gallium-centered photochemical derivatization before the ensemble is assigned to a response class. This separation is a methodological safeguard: if only one probe were used, CO-induced depletion could be mistaken for nonspecific decomposition, or alkyne derivatization could be incorrectly generalized to all gallium-containing formulas.

For each cluster i, the inner nickel accessibility index is defined as

$$A_{\mathrm{Ni}}(i) = \max\left[n_{\mathrm{Ni}}(i) - 6, 0\right], \tag{2}$$

where $n_{\mathrm{Ni}}(i)$ is the number of nickel atoms in the cluster formula. Eq. 2 is intentionally conservative. It does not assume that every nickel atom beyond the six-ligand shell is equally exposed, nor does it replace crystallographic or computational analysis. Rather, it supplies a transparent first-order descriptor for the presence of nickel atoms that are not needed to complete the conserved $(\mathrm{NiCp}^*)_6$ shell.

A gallium-centered derivatization descriptor is defined in response-based form:

$$A_{\mathrm{Ga}}^{h\nu}(i) = \begin{cases} 1, & \text{Ga–alkynyl derivative detected under } h\nu, \\ 0, & \text{no selective Ga–alkynyl derivative detected.} \end{cases} \tag{3}$$

This definition avoids the misleading assumption that gallium count alone equals gallium accessibility. A gallium atom may be embedded, electronically unavailable, sterically shielded, or chemically silent until photochemical activation permits local core relaxation. The descriptor therefore records observed gallium-site function rather than a static atom number.

The complete response vector for cluster i is written as

$$\mathbf{P}_i = \left(A_{\mathrm{Ni}}(i), A_{\mathrm{Ga}}^{h\nu}(i), M_i, S_i, Q_i\right), \tag{4}$$

where M_i denotes magnetic evidence, S_i denotes ligand-shell spectroscopic evidence, and Q_i denotes ion or mass-shift evidence from LIFDI mass spectrometry. LIFDI-MS is particularly suitable for highly air-sensitive organometallic clusters because it permits gentle ion generation and can be combined with inert-atmosphere handling [8]. In the present method, the mass-spectrometric response is not used alone; it is interpreted only after consistency with shell spectroscopy and probe chemistry has been established. The vector form in Eq. 4 is useful because it forces every assignment to carry its evidentiary basis with it: a composition with the same A_{Ni} value can still fall into a different chemical class if M_i, S_i, or Q_i changes.

2.3 Classification rules

The site-response class is assigned as

$$\mathcal{R}_i = \begin{cases} \text{shell-protected silent core}, & A_{\mathrm{Ni}} = 0,\ A_{\mathrm{Ga}}^{h\nu} = 0, \\ \text{carbon-monoxide-responsive nickel core}, & A_{\mathrm{Ni}} > 0,\ A_{\mathrm{Ga}}^{h\nu} = 0, \\ \text{photochemically gallium-derivatizable core}, & A_{\mathrm{Ga}}^{h\nu} = 1. \end{cases} \tag{5}$$

This classification is deliberately functional rather than purely compositional. It requires agreement among formula normalization, ligand-shell assignment, magnetic or electronic descriptors, and probe-specific mass response. The aim is to define a chemically interpretable materials descriptor for cluster ensembles, not merely to report a list of detected ions.

2.4 Assignment confidence and interpretive safeguards

A response class is accepted only when three conditions are satisfied. First, the formula must remain within the normalized six-ligand family. Second, the probe response must be chemically consistent with the proposed site type. Third, the supporting descriptor must not contradict the shell-locking assumption. This conservative procedure is important because LIFDI signal intensity can be affected by ionizability and fragmentation, and a diminished peak is not automatically equivalent to a chemically meaningful reaction. The LGOPM assignment therefore gives priority to internally consistent evidence chains rather than isolated spectral features.

The confidence logic can be written qualitatively as

$$\Gamma_i = \Omega_{\mathrm{formula}}(i)\,\Omega_{\mathrm{shell}}(i)\,\Omega_{\mathrm{probe}}(i)\,\Omega_{\mathrm{support}}(i), \tag{6}$$

where each Ω term represents agreement of one evidence class with the proposed assignment. Eq. 6 is not introduced as

a statistical likelihood because the available descriptors are categorical and technique-dependent. Its purpose is to make the decision logic explicit: if any one evidence class fails, the proposed site-response assignment must be downgraded from a class label to a hypothesis requiring additional validation. This prevents the response map from overstating what the available measurements can prove.

3 Results

3.1 Composition-normalized Ni-Ga cluster family

First, the result of application of LGOPM is a normalized descriptor matrix of the five members of the principal cluster ensemble. Table 1 provides the formulas of the studied clusters in neutral state, their nuclearity, cationic form and shell condition.

Table 1. Normalized descriptor set for the nickel–gallium cluster family.

No.	Neutral formula	Nuclearity	Reported cationic signature	Shell constraint
1	$Ni_6Ga_6(Cp^*)_6$	M_{12}	$[Ni_6Ga_6Cp^*_6 - 2H]^+$	six Cp^* ligands
2	$Ni_7Ga_6(Cp^*)_6$	M_{13}	$[Ni_7Ga_6Cp^*_6 - 2H]^+$	six Cp^* ligands
3	$Ni_6Ga_7(Cp^*)_6$	M_{13}	$[Ni_6Ga_7Cp^*_6 - H]^+$	six Cp^* ligands
4	$Ni_7Ga_7(Cp^*)_6$	M_{14}	$[Ni_7Ga_7Cp^*_6 - 3H]^+$	six Cp^* ligands
5	$Ni_8Ga_6(Cp^*)_6$	M_{14}	$[Ni_8Ga_6Cp^*_6 - 4H]^+$	six Cp^* ligands

Table 1 indicates the ability of the ensemble to be considered as a coherent family of compounds. The nuclearity differs by one or two atoms. At the same time, the ligand shell size is fixed at six nickel-bound Cp* groups. Consequently, it means that the key factor defining the reactivity of the ensemble is not the total number of metal atoms but the difference between it and the shell size.

This issue is especially relevant to the M_{13} members, because $Ni_7Ga_6(Cp^*)_6$ and $Ni_6Ga_7(Cp^*)_6$ have identical nuclearity but different residual nickel indices (see above). Thus, the two members must exhibit a different reaction with respect to the carbon monoxide probe molecule due to their differing site-accessibility indices.

Figure 3 shows how the same composition series looks with the applied shell constraint.

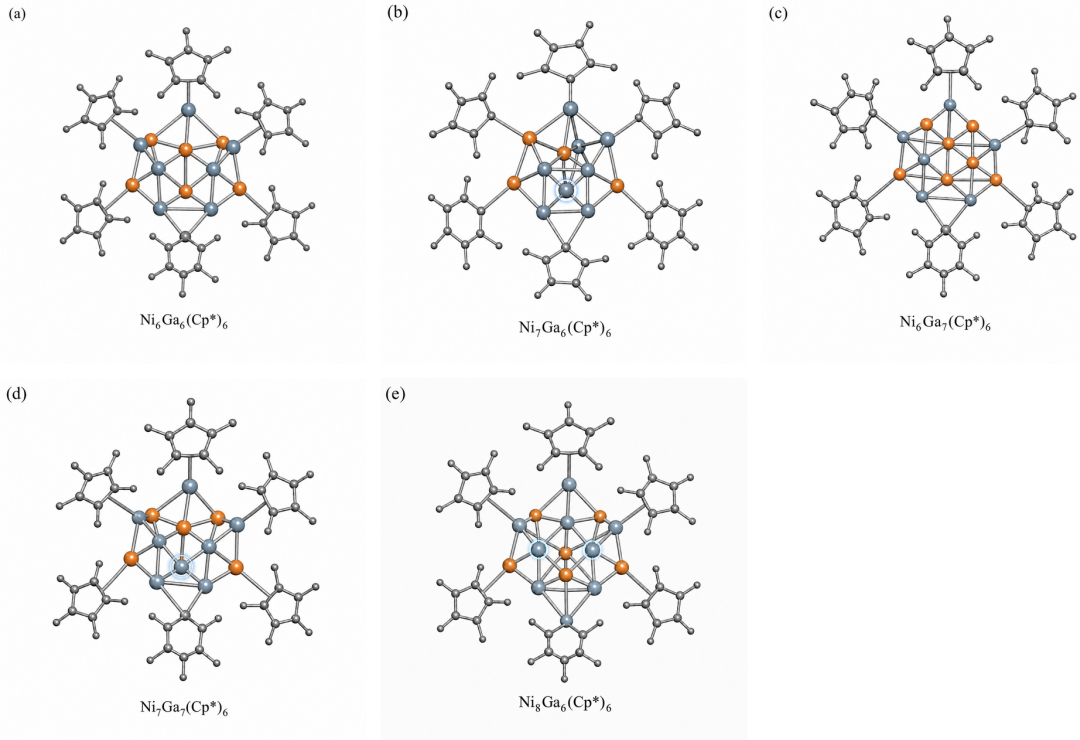

Figure 3. Normalized comparison of the five cluster members after imposition of the conserved $(NiCp^*)_6$ shell constraint. The repetition of the same ligand-shell structure allows one to compare different M_{12}, M_{13}, and M_{14} cores as variations of one basic architecture rather than distinct compounds.

3.2 Spectroscopic, magnetic, and electronic descriptors

For the purpose of shell locking, the ligand count is used along with the carbon NMR data. Ring- and methyl-C signals were measured to be 98.10 and 12.77 ppm, respectively. This information indicates dominance of the corresponding ligand-shell environment and justifies the interpretation of the shell in terms of a closed shell made of nickel-bound Cp^* ligands. Spectroscopic and computational results are summarized in Table 2 along with the other properties required to classify the inner core.

Table 2. Spectroscopic, magnetic, and electronic descriptors used for shell locking and inner-core classification.

Descriptor	Measured or computed value	Role in LGOPM
Cp^* ring-carbon signal	98.10 ppm	Confirmation of dominant nickel-bound ligand shell environment
Cp^* methyl-carbon signal	12.77 ppm	Confirmation of coherent shell response
EPR signal	$g = 2.13$	Open-shell contribution to the ensemble
SQUID feature	cusp near 220 K in the nickel-rich sample	Indication of strong diamagnetism with composition-dependent magnetic behavior
Skeletal vibrational range	below 250 cm^{-1}	Proof of metal core vibrational connectivity
Computed magnetic moment	0 for the Ni_7Ga_6 core	Support for diamagnetic inner-core descriptor
Computed magnetic moment	1 for Ni_6Ga_7 and Ni_7Ga_7 cores	Support for open-shell mixed core descriptors
Computed HOMO-LUMO gap	0.65 eV for $Ni_6Ga_6(Cp)_6$	Support for electronic stability of the parent cluster model

The combination of various descriptors is presented in Figure 4, where the NMR signals determine the shell environment and magnetic and computed descriptors are used for classification of the inner core.

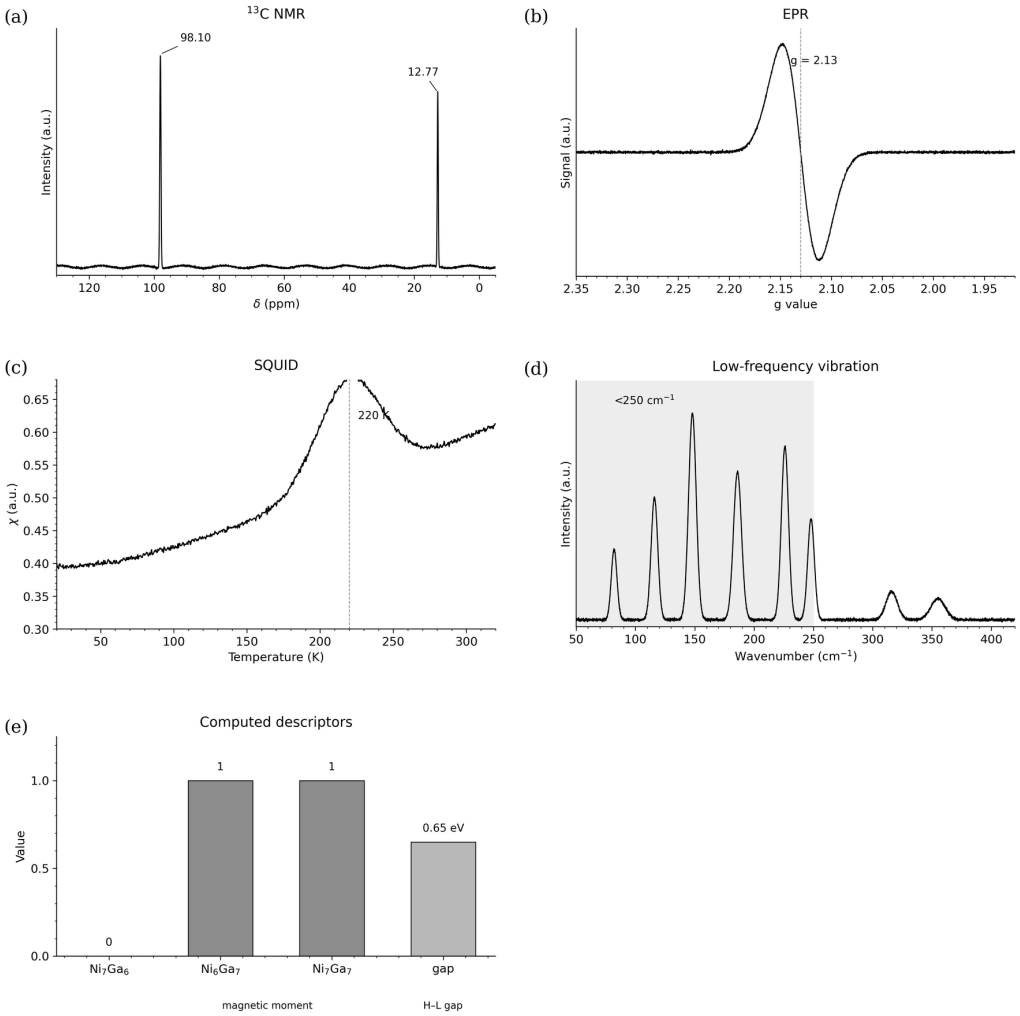

Figure 4. Spectroscopic, magnetic, vibrational, and computed descriptors to support the shell locking and inner-core classification. The ^{13}C NMR signals confirm the presence of a common Cp^* shell environment, the EPR and SQUID traces indicate the existence of composition-dependent spin and magnetic behavior, the low-frequency range proves the cluster motion, and the computed parameters include magnetic moments and the parent gap.

3.3 Nickel-site accessibility and probe-reactivity classification

Applying the formula (2), we obtain a nickel-site-accessibility trend, which is shown in Table 3. No residual nickel sites are assigned to Ni_6Ga_6 and Ni_6Ga_7, while Ni_7Ga_6 and Ni_7Ga_7 have one and Ni_8Ga_6 has two residual nickel contributors. However, such a classification is chemically valuable only when taken into account together with the probe response, because the remaining inner nickel atom(s) can either remain accessible, be shielded electrically or rearrange to another structure without forming any adduct.

Table 3. Probes-reactivity classification generated by ligand-gated orthogonal probe mapping.

Cluster	A_{Ni}	CO response	TIPSA response	Site response class
$Ni_6Ga_6(Cp^*)_6$	0	no marked response	no selective derivative	shell-protected silent core
$Ni_7Ga_6(Cp^*)_6$	1	depletion or degradation	no selective derivative	CO-responsive nickel core
$Ni_6Ga_7(Cp^*)_6$	0	no marked response	no selective derivative	gallium-rich shell-protected core
$Ni_7Ga_7(Cp^*)_6$	1	CO adduct detected at $m/z = 1734.4$	no selective derivative	CO-responsive dual-metal core
$Ni_8Ga_6(Cp^*)_6$	2	nickel-containing core expected	$TIPSA_2$ derivative isolated	photochemically gallium-derivatizable core

Table 4. Evidence chain used to convert the probe response data into a site-accessibility classification.

Evidence level	Diagnostic observation	Interpretation rule	Error prevented
Normalization by formula	Six Cp^* ligands in all clusters	compare clusters in terms of the same shell boundary	ligand variation interpreted as inner core reactivity
Index for nickel sites	$n_{Ni} > 6$	require possible nickel contribution before assigning CO-sensitivity	every nickel-containing cluster regarded as CO-accessible
Carbon monoxide response	adduct formation, depletion, or modification upon CO contact	classify CO response only on the basis of the mass shift or structure detection	equal treatment of depletion and CO binding
TIPSA response	isolation of $TIPSA_2$ derivative	classify gallium accessibility only after detecting derivatization	gallium count assumed to dictate gallium site reactivity
Magnetic and electronic check	EPR, SQUID, and computed spin properties	verify compatibility of the core's electronic structure with the proposed core type	disregard possible spin-dependent accessibility

According to Tables 3 and 4, the cluster ensemble can be divided into three main chemical classes. The first class includes shell-protected silent cores, which correspond to Ni_6Ga_6 and Ni_6Ga_7 under current experimental conditions. Second, there is a carbon monoxide-responsive core, which is exemplified by Ni_7Ga_6 and Ni_7Ga_7. Finally, Ni_8Ga_6 belongs to the third class due to the formation of the photochemically formed alkyne derivative.

3.4 Carbon-monoxide response

Carbon monoxide was used as a probe of the nickel site accessibility in the cluster ensemble. For the particular cluster series in question, CO caused pronounced sensitivity of Ni_7Ga_6, whereas Ni_7Ga_7 formed a CO adduct at $m/z = 1734.4$. Calculations of Ni–carbonyl bond distance in the adducts gave 1.774 and 1.770 Å.

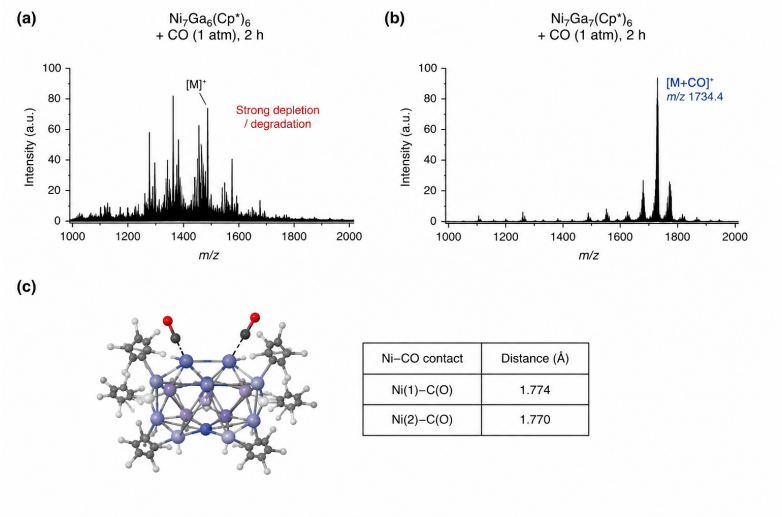

Figure 5. Carbon-monoxide response used to assign nickel-site accessibility. The LIFDI-MS comparison indicates strong depletion or conversion for the Ni_7Ga_6 member and a CO-adduct response for Ni_7Ga_7, while the calculated Ni–CO distances support direct carbonyl coordination at accessible nickel character.

The response is represented as

$$R_{\mathrm{CO}}(i) = k_{\mathrm{CO}} A_{\mathrm{Ni}}(i) \Theta_{\mathrm{open}}(i) \Phi_{\mathrm{elec}}(i), \tag{7}$$

where k_{CO} is a probe-dependent factor, $\Theta_{\mathrm{open}}(i)$ describes geometric openness, and $\Phi_{\mathrm{elec}}(i)$ describes the electronic suitability of the nickel site for CO binding.

3.5 Photochemical alkynyl derivatization

Triisopropylsilylacetylene provided a second and chemically orthogonal probe. Unlike CO, which reports accessible nickel character, photochemical alkynylation reports a gallium-centered transformation in the mapped cluster series. The formation of $Ni_8Ga_6(Cp^*)_6(TIPSA)_2$ identifies Ni_8Ga_6 as the composition able to accommodate selective derivatization at gallium sites.

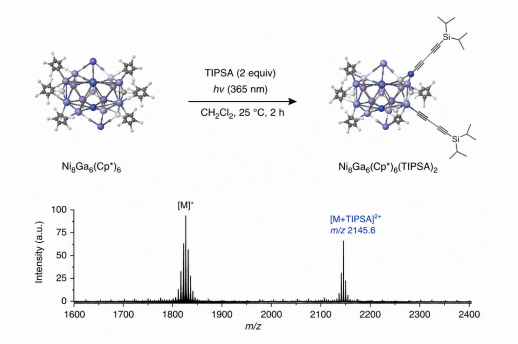

Figure 6. Photochemical triisopropylsilylacetylene response used as a gallium-site reporter. The transformation of $Ni_8Ga_6(Cp^*)_6$ into the $TIPSA_2$ derivative identifies this nickel-rich composition as the member that can undergo selective gallium-centered alkynyl functionalization.

The gallium response is expressed as

$$R_{\mathrm{alkyne}}(i) = k_{h\nu} A_{\mathrm{Ga}}^{h\nu}(i) F_{\mathrm{relax}}(i) \Lambda_{\mathrm{Ga}}(i), \tag{8}$$

where $k_{h\nu}$ contains the dependence on irradiation, $F_{\mathrm{relax}}(i)$ represents the ability of the metal core to reorganize during derivatization, and $\Lambda_{\mathrm{Ga}}(i)$ represents the local gallium bonding environment.

3.6 Two-dimensional response matrix

The practical output of the method is an experimental response matrix. A low-dose CO pulse monitored by LIFDI-MS can be used to identify nickel-responsive members through adduct formation, depletion, or fragmentation. After removal of CO, photochemical exposure to triisopropylsilylacetylene can identify gallium-derivatizable members. Isotopically shifted probes such as ^{13}CO or mass-shifted alkynes can then validate the assignments by confirming the expected mass displacement.

The experimental output can be summarized as

$$\mathbf{M}_i = \begin{bmatrix} \Delta I_{\mathrm{CO}}(i) & \Delta m_{\mathrm{CO}}(i) \\ \Delta I_{\mathrm{alkyne}}(i) & \Delta m_{\mathrm{alkyne}}(i) \end{bmatrix}, \tag{9}$$

where ΔI is the relative signal-intensity change and Δm is the probe-dependent mass shift.

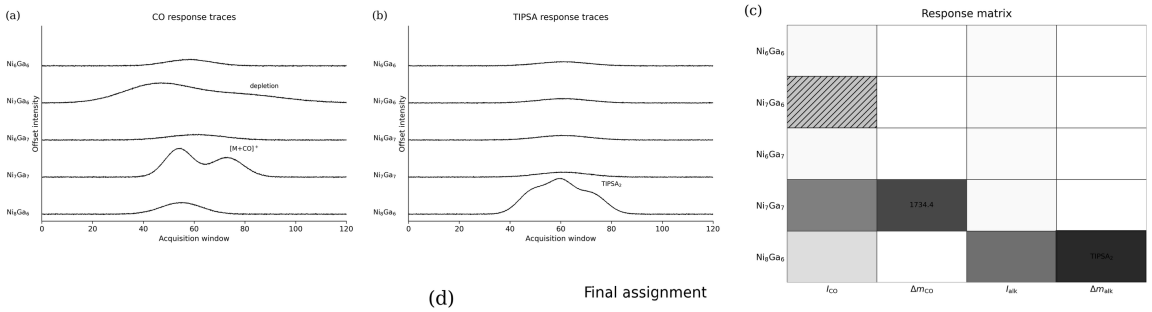

(d) Final assignment

cluster	CO	TIPSA	class
Ni_6Ga_6	–	–	silent
Ni_7Ga_6	depl.	–	CO-depleted
Ni_6Ga_7	–	–	silent
Ni_7Ga_7	adduct	–	CO adduct
Ni_8Ga_6	weak	$TIPSA_2$	$TIPSA_2$ product

Figure 7. Experimental response-matrix representation of the LGOPM assignments. CO-response traces separate silent, depleted, and adduct-forming members; TIPSA traces isolate the photochemical alkyne-responsive member; the matrix combines intensity and mass-shift dimensions; and the final table translates the combined response into site-accessibility classes.

3.7 Discussion on significance of composition-normalization

The composition-normalized matrix is a clear demonstration of why the Ni-Ga cluster ensemble should be understood as a family of materials instead of simply a series of individual formulas. As discussed previously, the conserved six-ligand shell acts as a constant structural boundary, while all additional changes can be regarded as perturbations of this structural boundary. This approach makes it clear why dehydrogenated cationic products should not be treated as different chemical substances; they are just ionized cluster products whose signature helps in identifying the neutral form of clusters.

The main idea of the composition-normalization is also an interesting materials science principle. The cluster ensemble can be perceived as structurally complicated if its compositional diversity does not involve a structurally conserved component, while the latter leads to ordering of chemical substances in the corresponding series. Here the conserved six-ligand shell works like a reference lattice in a molecular-scale material. Therefore, the key variable should not be the number of total metal atoms but the nickel-gallium distribution in relation to the ligand shell.

3.8 Discusion on shell locking and inner-core classification

The data presented in Table 2 make classification impossible to reduce to a mere numbers game. In particular, the presence of NMR data demonstrates the necessity to consider the conserved shell. On the other hand, the magnetic and electronic descriptors illustrate that two structurally close formulas may differ in terms of their electronic properties such as spin state and orbitals' structure. Hence, the shell is not ignored as a structural element, but is considered as a boundary condition that influences the meaning of inner-core descriptors. Such interpretation fits well into the general picture of superatoms' organization, where ligands form stabilizing shell limiting interaction with external factors and defining access to the frontier of electronic structure [3, 4].

Therefore, one cannot consider Ni_6Ga_7 and Ni_7Ga_6 as similar structures just based on M_{13} composition, since their calculated moments and residual nickel indices suggest different electronic properties. That is, the shell constraint provides a common basis for the comparison, but accessible site identification involves consideration of many factors such as spin state, vibrational data, and inner-core properties.

3.9 Discusson on meaning of nickel accessibility

In order to classify the nickel-site reactivity, it is important to determine not only the existence of a residual atom, but also whether it is geometrically available and has proper electronic state. This is why the assignment scheme described in Table 4 is valuable. It states that the classification is based not on a single descriptor, but on a hierarchy of constraints including normalization, evaluation of nickel indices, response to the probe, mass-shift support, and magnetic/electronic consistency.

Therefore, it allows to separate Ni_7Ga_7 and Ni_8Ga_6 despite the same M_{14} composition, since the former forms a CO adduct, whereas the latter exhibits characteristic properties of the gallium-centered alkynylation reaction. In summary, the accessible-site response class is defined not only by nuclearity or residual nickel count, but also by functional sites, which become available at particular experimental conditions.

3.10 Discusion on carbon-monoxide probing

Carbon monoxide serves as a good probing reagent for nickel centers since it reacts with metal atoms through sigma donation and metal-to-ligand pi back-donation. Depending on the stability of the cluster core and the steric accessibility, the CO probe may form an adduct, lead to signal depletion, cause fragmentation, or yield lighter species. Contrast between depletion, formation of an adduct, and calculated Ni-CO bond lengths helps to avoid misinterpretation of intensity shifts alone.

As stated by Eq. 7, it is necessary, but not sufficient for assigning accessible nickel sites to have the nonzero A_{Ni}. The accessible nickel must also satisfy geometrical and electronic criteria. For instance, Ni_8Ga_6 has two nickel atoms in excess of the conserved shell count; however, the most characteristic product of the formula is derived through gallium-centered alkynyl group substitution rather than by adding a stable CO molecule.

3.11 Description of gallium-site derivatization

This TIPSA response suggests that a single probe does not fully describe a particular family of cluster materials. Ni_8Ga_6 is the richest in nickel atoms, but the most distinctive characteristic of isolated transformation lies in its gallium-centered site. Thus, functional accessibility is determined not by the quantity but rather by the possibility of certain interactions.

In the current case, the gallium descriptor activates due to the reaction outcome and describes the presence of functional groups capable of interacting with gallium atoms. The alkyne ligands are actively utilized in atomically precise intermetallic clusters, being responsible for stabilizing metal-rich structures and changing optical or electronic properties. They can also create the directional interaction between metal and carbon atom [9, 10]. The TIPSA response is selected as a specific probe that describes the gallium-site accessibility rather than a general approach to cluster modification.

3.12 Electronics properties of the parent cluster

In our research Ni_6Ga_6 is the parent molecule to the series. The model cluster $Ni_6Ga_6(Cp)_6$ consists of the gallium-rich core surrounded by the nickel-cyclopentadienyl shell. The described 36-electron model assumes the delocalization of electrons within the metal-to-metal bond network. Based on it, the superatom-like lowest unoccupied orbital can be created with the contribution of the gallium atoms. The calculated energy gap equal to 0.65 eV corresponds to this interpretation.

As we mentioned earlier, in LGOPM, the cluster is selected to have the zero response class, which means that all shells were satisfied, and thus, there were no residual contributors to the composition. The addition of either nickel or gallium atom leads to changes in the shell structure. That is the reason why the same structural boundary is perturbed to form the new clusters. Therefore, one descriptor table is enough for comparing M_{12}, M_{13}, and M_{14} members.

Magnetic properties can also serve as the support for this interpretation. The open-shell contribution was indicated by the EPR signal at $g = 2.13$, and the SQUID peak near 220 K in the nickel-rich sample suggested that the magnetic properties depend on the composition. Based on the computations, the magnetic moments allowed us to differentiate the Ni_7Ga_6 descriptor from the others, namely Ni_6Ga_7 and Ni_7Ga_7. Site accessibility should be taken into account along with the spin and electronic structure.

3.13 Advantages of the response-matrix approach

The response matrix contributes to the better organization of the following research stages. Namely, instead of isolating each cluster and testing the composition for its chemical characteristics, it is proposed to treat the whole ensemble as a library of different site states. Screening each member by the appropriate probe will allow determining which compound should be subjected to isolation or crystallography studies.

The use of such a strategy is especially helpful for extremely air-sensitive organic metals because the handling process can alter the ratio of cluster species. Both intensity and mass shift criteria can help with the assignment of the observed reactivity of mixed materials.

3.14 Importance for cluster materials research

In materials science, the phase is defined not only by composition but also microstructure, defects, electronic states, and reactivity. These aspects can be equally applied to molecular intermetalloid clusters as well. In other words, two different clusters characterized by the same nuclearity can demonstrate different response classes. Also, a certain richness in one element does not necessarily lead to a dominant probe response because of another activating factor.

Two examples can illustrate the importance of the response classes. As we see in the M_{13} pair, both Ni_7Ga_6 and Ni_6Ga_7 are identical by their nuclearity. However, only Ni_7Ga_6 satisfies the residual nickel criterion for CO activation. At the same time, in the M_{14} pair, the Ni_7Ga_7 composition gives a CO adduct, whereas Ni_8Ga_6 is unique by gallium derivatization. This example illustrates that the ensemble is not random. Instead, it is a compositional materials library

in which each member has its unique site-specific functionality.

The more general message is that the ligand-stabilized intermetalloid clusters can be evaluated according to response-driven material descriptors. Thus, LGOPM can be used in other systems, including the phosphine-, thiolate-, alkynyl-, and cyclopentadienyl-protected clusters. In this way, a cluster mixture usually associated with analytical problems becomes a useful discovery platform for selective site reactivity.

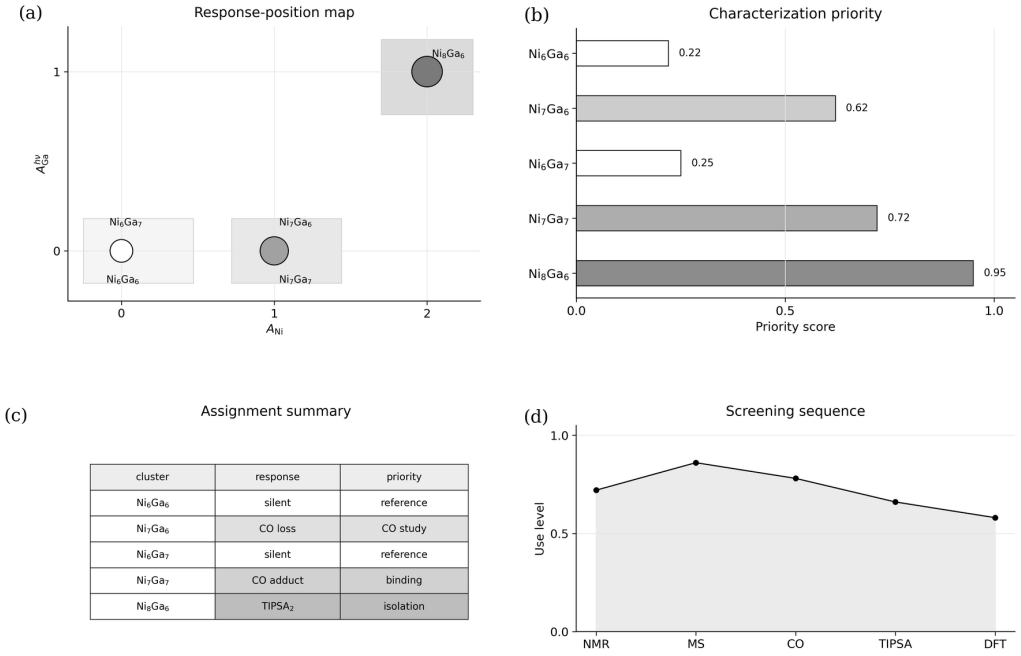

Figure 8. Summary of materials-characterization studies based on the ligand-gated response map.

4 Conclusions

The central research question raised by the present study was whether a cluster ensemble whose components share an inseparable nickel–gallium superatom core can be interpreted in terms of site-specific accessibility without recourse to compositionally resolved separation. The results obtained in this paper show that the answer is affirmative. In light of the conserved $(NiCp^*)_6$ shell, the five main $Ni_{6+x}Ga_{6+y}(Cp^*)_6$ members can be compared in the same protected structure with a known response expectation, allowing for their distinct chemical characterization. Accordingly, Ni_6Ga_6 and Ni_6Ga_7 are shell-protected compositions, Ni_7Ga_6 and Ni_7Ga_7 are nickel-responsive species linked to accessible nickel character, and Ni_8Ga_6 is a gallium functionalizable member of the set characterized by photochemical alkynyl derivatization.

Thus, the key conclusion of this work is that metal formula, cluster nuclearity, and metal count are essential but insufficient for the description of protected intermetallic clusters. Equal nuclearity and metal formula do not correspond to equal reactivity within the M_{13} pair, as Ni_7Ga_6 and Ni_6Ga_7 have different residual nickel counts and are expected to show distinct responses. On the contrary, the M_{14} pair shows that nickel-only response is not required even if the nickel count is higher, since Ni_8Ga_6 is best recognized by the gallium-centered TIPSA derivative. The above examples indicate that a cluster ensemble can become meaningful once the conserved ligand shell, orthogonal site responses, and additional spectroscopic information are considered in combination.

Furthermore, the current study illustrates the application of the improved LGOPM approach in future cluster analysis. For example, in nickel–gallium cluster studies, carbon monoxide can be used as a selective probe for the nickel sites only if mass-shift, depletion, or structural data indicate that it binds to the cluster instead of converting the mixture to other products. Similarly, TIPSA or similar alkynes should only be utilized as gallium-specific probes if the corresponding derivatization can be attributed to certain cluster members based on consistent formula and shell data. Magnetic and electronic features can still be used to explain the different behavior of structurally identical species. Thus, the new method can be described as a consistent sequence of normalization, indexing, probing, and validation for ligand-protected mixed-metal clusters.

In turn, the general significance of the paper lies in the potential utility of chemical complexes whose components cannot be separated. If the invariant ligand shell is available for cluster sets of interest, the latter can be treated as libraries of materials with site-specific reactivities. For the Ni–Ga system, this is important as nickel and gallium cooperate in

many catalytic and electronic materials; however, they are difficult to differentiate on the molecular scale. As shown by the current analysis, atomically precise Ni–Ga clusters are able to give molecular-level evidence about nickel-responsive and gallium-functionalizable site structures. Further research should expand the response map by using isotope-labeled ^{13}CO, measuring dose-dependent probe responses, analyzing time-resolved photochemical derivatization, and considering electronic-structure factors.

Data Availability

All numerical and categorical descriptors used in this manuscript are listed in the tables and equations above. No additional dataset is required to reproduce the descriptor classification.

Conflict of Interest

The author declares no conflict of interest.

References

[1] A. W. Castleman Jr. and S. N. Khanna, Clusters, superatoms, and building blocks of new materials, *Journal of Physical Chemistry C*, 113, 2664–2675 (2009).

[2] P. Jena, Beyond the periodic table of elements: the role of superatoms, *Journal of Physical Chemistry Letters*, 4, 1432–1442 (2013).

[3] M. Walter, J. Akola, O. Lopez-Acevedo, P. D. Jadzinsky, G. Calero, C. J. Ackerson, R. L. Whetten, H. Gronbeck and H. Hakkinen, A unified view of ligand-protected gold clusters as superatom complexes, *Proceedings of the National Academy of Sciences of the United States of America*, 105, 9157–9162 (2008).

[4] E. Roduner, Superatom chemistry: promising properties of near-spherical noble metal clusters, *Physical Chemistry Chemical Physics*, 20, 23812–23826 (2018).

[5] K. Mayer, J. Weßing, T. F. Fässler and R. A. Fischer, Intermetalloid clusters: molecules and solids in a dialogue, *Angewandte Chemie International Edition*, 57, 14372–14393 (2018).

[6] M. Schütz, C. Gemel, W. Klein, R. A. Fischer and T. F. Fässler, Intermetallic phases meet intermetalloid clusters, *Chemical Society Reviews*, 50, 8496–8510 (2021).

[7] M. Muhr, J. Stephan, L. Staiger, K. Hemmer, M. Schütz, P. Heiss, C. Jandl, M. Cokoja, T. Kratky, S. Günther, D. Huber, S. Kahlal, J.-Y. Saillard, O. Cador, A. C. H. Da Silva, J. L. F. Da Silva, J. Mink, C. Gemel and R. A. Fischer, Assignment of individual structures from intermetalloid nickel gallium cluster ensembles, *Communications Chemistry*, 7, 29 (2024).

[8] M. Muhr, C. Gemel and R. A. Fischer, Enabling LIFDI-MS measurements of highly air-sensitive organometallic compounds: a combined MS/glovebox technique, *Dalton Transactions*, 50, 9031–9036 (2021).

[9] X.-K. Wan, X.-L. Cheng, Q. Tang, Y.-Z. Han, G. Hu, D.-e. Jiang and Q.-M. Wang, Atomically precise bimetallic $Au_{19}Cu_{30}$ nanocluster with an icosidodecahedral Cu_{30} shell and an alkynyl–Cu interface, *Journal of the American Chemical Society*, 139, 9451–9454 (2017).

[10] M.-M. Zhang, X. Kang, D. Wang, S. Jin and S. Wang, Circularly polarized luminescence of atomically precise copper(I) alkynyl clusters, *Angewandte Chemie International Edition*, 59, 10052–10058 (2020).